

The Reliability of Extreme Surge Levels, Estimated from Observational Records of Order Hundred Years

H.W. van den Brink, G.P. Können, and J.D. Opsteegh

Royal Netherlands Meteorological Institute
KNMI
P.O. Box 201
3730 AE De Bilt
The Netherlands

ABSTRACT

VAN DEN BRINK, H. W.; KÖNNEN, G. P., and OPSTEEGH, J. D., 2003. The reliability of extreme surge levels, estimated from observational records of order hundred years. *Journal of Coastal Research*, 19(2), 376–388. West Palm Beach (Florida), ISSN 0749-0208.

General Circulation Model-generated surges are analyzed with the Generalized Extreme Value distribution to study the uncertainty in surge level estimates with a return period of 10^4 years, derived from observational records of order hundred years.

Ensemble simulations with a total length of 5336 years were generated with the KNMI General Circulation Model ECBilt, coupled with a simple surge model to transform the wind field over the North Sea to the surge level at Delfzijl (NL). The 46 estimated surge levels with a return period of 10^4 years, calculated from sets of 116 year each, vary between 4.5 and 17 meters, with a median of 8.5 meter. The 10^4 -year estimate of the 118-year observational Delfzijl record (5.8 meter) fits well among these subsets, but this surge level is considerably lower than the median of the ensemble estimate. For an estimate of the 10^4 -year return level of the surge within an uncertainty of 10%, a record length of about 10^3 years is required.

CO₂-doubling does not have a detectable influence on the mean wind speed over the North Sea in ECBilt. However, the model hints on the excitation of severe storms, with a frequency lower than once in 250 year. In ECBilt, these severe storms tend to dominate the 10^4 -year return value of the wind speed over the North Sea.

ADDITIONAL INDEX WORDS: *Extreme value statistics, surge, uncertainty, climate change.*



INTRODUCTION

Protection of the Netherlands against flooding from the sea is a matter of continuous concern. In coastal protection, a probability of 10^{-4} per year for flooding from the sea is used as baseline (DELTACOMMISSIE, 1960). The determination of the corresponding design height of the dikes requires knowledge about the tides and surges. Tides are deterministic, but surges are wind-driven, and hence stochastic.

Several problems arise when the 'accepted risk' has to be translated into the surge level being exceeded (on average) only once in 10^4 years. First, as the observational records of skew surges are only 10^2 years in length, the surge level with an average return period of 10^4 years requires an extrapolation of two orders of magnitude. It is unclear how reliable the estimate from such an extrapolation is. Second, various probability functions can be fitted to the observational records of extreme surges, leading to different results in the 10^4 -year return levels (DILLINGH *et al.*, 1993; DE HAAN, 1990). Third, extrapolation from observational records does not contain in-

formation about surges in a greenhousegas-induced changing climate.

These problems can be explored by using a long surge record (in the order of 10^4 years) generated by a climate model. From this record, the most adequate extreme-value distribution can be determined, as well as its parameter values and the 10^4 -year surge level (within the context of the model). This most adequate distribution can then be applied to subsets of the long record, each with a time length equal to the available observational records (~ 100 years). The variation in the estimated parameter values and in the 10^4 -year surge level among the subsets provides information about the uncertainty of the estimate from the observational record.

This procedure has been applied using current climate data of the KNMI climate model ECBilt. We have concentrated on the model grid point best representing the wind field over the North Sea, and applied the surge model to the coastal station Delfzijl (NL). The effect of an increased greenhousegas concentration on extreme wind speeds is preliminary investigated.

Our study can be regarded to be complementary to studies on changing wind climate using state of the art GCMs (KHARIN and ZWIERS, 2000; BEERSMA *et al.*, 1997; KNIPPERTZ *et al.*, 2000; SCHUBERT *et al.*, 1998; HALL *et al.*, 1994). These studies have in common that they are based on output of limited length (typical 5 to 50 years), an unavoidable conse-

02073 received and accepted 6 June 2002.

The research is partly carried out in the framework of the Dutch National Research Programme on Global Air Pollution and Climate Change, registered under No. 951269, and partly funded by the Dutch National Institute for Coastal and Marine Management (RIKZ), registered under No. RKZ1006.

quence of the complexity of these models. The limited length prevents examination of a possible change in extremes of return periods of thousands of years. In the present study, a simpler model is used, which enabled us to generate $5 \cdot 10^3$ years for the greenhouse climate at CO_2 doubling, and to explore the properties of the extreme value statistics up to return periods of 10^4 year within the context of this model, but using a meteorological parameter (surge) that is generated by a wind field of time and spatial scales comparable with the (coarse) grid distance of that model.

The paper is structured as follows: Section 2 describes the models used, and Section 3 the theoretical and experimental design. The validation of the data and models used is given in Section 4. Section 5 gives the results, and Section 6 the discussion and conclusions.

MODEL DESCRIPTIONS

Climate Model

The wind data are produced by a General Circulation Model (GCM) of intermediate complexity. A GCM calculates the time evolution of a large number of weather variables on a discrete grid. For this calculation, the equations of fluid flow on a rotating earth are solved on this grid, while sub-grid physical processes are parameterized. In this way, meteorological quantities can be derived for very long periods. Because of the chaotic nature of the atmosphere, the results do not have deterministic forecast-value, but the sub-daily output does provide statistical information about the climate properties of the model.

In this study, the GCM of the KNMI, called ECBilt, was used. The atmospheric component of ECBilt is a spectral T21 global 3-level quasi-geostrophic model. The T21-resolution corresponds (for the latitudes of interest) with a grid point distance of approximately 500 km. The atmospheric time step is 4 hours. The atmospheric component of the model is coupled to a simple ocean-GCM and a thermodynamic sea-ice model. ECBilt is two orders of magnitude faster than state-of-the-art GCMs, providing the possibility of studying climate dynamics on time scales of thousands of years. For a detailed description of ECBilt we refer to OPSTEEGH *et al.* (1998, 2001).

Surge Model

The sea level at a certain position and time is determined by a combination of two effects: the astronomical tide and the surge. The surge is the difference between the actual level and the astronomical tide. Neglecting resonances and other second-order effects, the surge is determined by the wind and the pressure. Whereas the astronomical tide is deterministic, the meteorological effect is stochastic.

Usually, calculated (or forecasted) surges are verified against observations of the so-called skew surge. The skew surge at high (low) tide is the difference between the astronomical high (low) tide and the observed high (low) tide. Due to hydraulic effects, the observed and astronomical high tides do not necessarily occur at the same moment (see Figure 1), particularly when the surges are large. Most surge models do

not take this effect into account. The problems arising in the calculation of the surge from time-lagged astronomical tidal curves are bypassed by verification on the skew surge. Usually, the high tide (rather than the low tide) skew surges are considered, restricting the number of verification moments to two per day. In practice, the observed skew surge is compared with the calculated surge for the moment of astronomical high tide. In the validation of our model, we adopted this procedure.

The relation we used to model the skew surge is based on the semi-empirical Timmerman model (TIMMERMAN, 1977). This surge model was used for many years at KNMI for operational surge forecasting. We simplified this model by neglecting time- and space-dependencies, and assuming a sinusoidal dependence on the wind direction. This results in the following relation for the skew surge:

$$y = \gamma u^2 \cos(\phi - \beta) + \frac{1013 - p}{100.5} \text{ [m]} \quad (1)$$

The first term is the wind effect, with u the wind speed and ϕ the clockwise wind direction with respect to north. The station pressure p is in mbar. The station-dependent parameters γ and β are determined by fitting Eq. 1 to the time- and space-averaged values, given by TIMMERMAN (1977) for the station considered. For Delfzijl, $\gamma = 5.5 \cdot 10^{-3} \text{ s}^2 \text{ m}^{-1}$ and $\beta = 321^\circ$. So, the surge is maximal for North Western winds. For extreme surges, the second term in Eq. 1, which is the barometric pressure effect, is neglected, as it has a constant value of only 10 cm (see Section 4.1).

The surge is calculated every 12 hours from the wind averaged over the last 3 time steps (of 4 hours) of the ECBilt model. The choice for averaging over 12 hours has three reasons. First, the mean time lag between the wind over the North Sea and the surge at the coast is 6 hours, being of the same order. Second, the Timmerman model also uses time-averaged values, to incorporate the inertia of the surge phenomenon. Third, the periodicity of the tide is close to 12 hours.

Calculations are also done with the NCEP reanalysis wind data. Figure 2 shows the ECBilt and NCEP grid points.

We found that, for our experimental set-up, the intermediate complexity of ECBilt lends itself optimally to the calculation of the 10^4 -year surge level, as on the one hand ECBilt is fast enough to generate thousands of years of wind data, and on the other hand it provides the large-scale wind, which drives the surge.

METHODOLOGY

Generalized Extreme Value Distribution

We applied the Generalized Extreme Value (GEV) distribution to the set of annual maxima of the surge and the wind speed to describe the statistical properties of the extremes. The distribution of normalized extremes approaches asymptotically to this GEV distribution (see *e.g.* DE HAAN (1976), GALAMBOS (1978) and KOTZ and NADARAJAH (2000)), which is described analytically by:

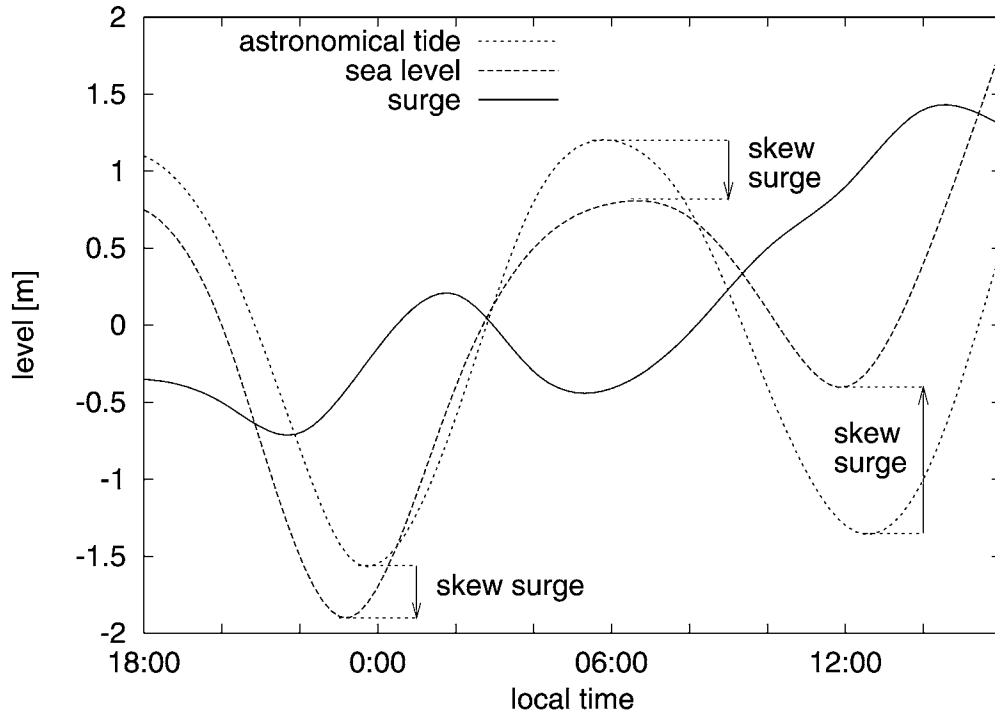


Figure 1. The surge (solid line) is the difference between observed sea level and astronomical tide at each moment. Due to hydraulic effects, the tidal curve may be shifted with respect to the astronomical tide. This leads to spurious effects in the surge. Surge predictions are therefore verified against the skew surge, which is the difference between the astronomical high (low) tide and the associated observed high (low) tide, which need not to take place at the same moment. In the figure the skew surges at the first low tide (0:00) and the high tide (6:00) are negative, whereas the second low tide skew surge (12:00) is positive (indicated with arrows). Shown is the situation at Delfzijl from 21 Feb 2002 18:00 to 22 Feb 2002 16:00 local time.

$$F(y) = e^{-e^{-x}} \tag{2}$$

where x is a substitute for:

$$x = \ln \left[1 - \frac{\theta}{\alpha} (y - \mu) \right]^{-1/\theta} \tag{3}$$

with μ the location parameter, α the scale parameter, θ the shape parameter, and y the variable considered (JENKINSON, 1955). These parameters are indicated in Figure 3. Depending on the sign of θ , 3 types are distinguished:

1. $\theta = 0$; The Gumbel or Fisher-Tippett I distribution
2. $\theta < 0$; The Fisher-Tippett II distribution, having a lower limit
3. $\theta > 0$; The Fisher-Tippett III distribution, with an upper limit

For the Gumbel distribution ($\theta = 0$), Eq. (3) can be simplified to:

$$x = \frac{y - \mu}{\alpha} \tag{4}$$

The probability of exceedance of a certain level is usually expressed in terms of the return period T . The *return period* T is the average number of years between two succeeding exceedances of the corresponding *return level* y :

$$T(y) = \frac{1}{1 - F(y)} = \frac{1}{1 - e^{-e^{-x}}} \tag{5}$$

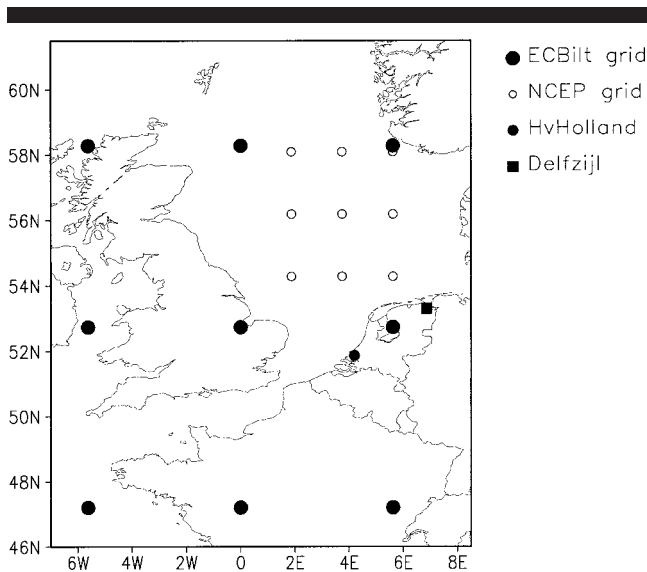


Figure 2. The grid points of EC Bilt and NCEP. From the NCEP grid, only the grid points used for validation are shown. The Dutch coastal stations Hoek van Holland and Delfzijl are indicated.

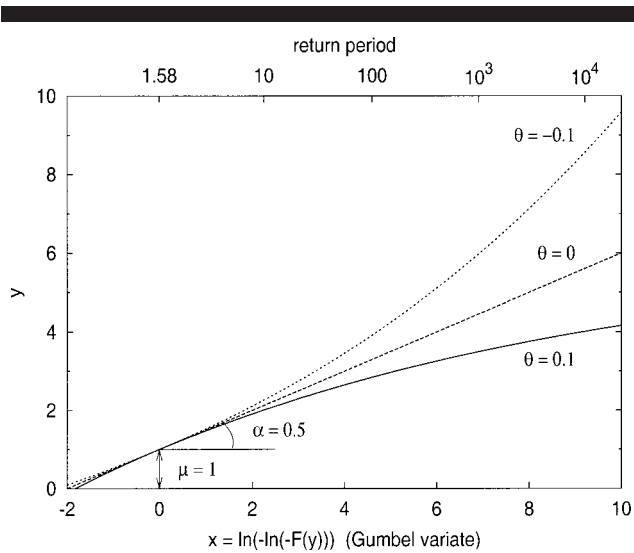


Figure 3. The parameters of the GEV distribution. The location parameter μ is the value corresponding with $x = 0$ and $T = 1.58$. The scale parameter α is the slope at $x = 0$, and the shape parameter θ is the curvature. For large return periods, y strongly depends on θ .

An estimate of $F(y)$ is obtained by using the ordered extremes $y_1 \leq y_2 \dots \leq y_n$. The n extremes divide the total range between 0 and 1 into $n + 1$ equally spaced intervals, and thus $E\{F(y_i)\} = i/(n + 1)$ (VAN MONTFORT, 1969).

A plot of the ordered extremes y_i against the Gumbel variate $x_i = \ln(-\ln(-E\{F(y_i)\}))$ (a so-called Gumbel plot) will result in a straight line if the distribution obeys the Gumbel distribution, or in a curved line—convex for type II and concave for type III (see Figure 3). For a more comprehensive description we refer to KOTZ and NADARAJAH (2000). The above property analysis—convergence of extremes to the GEV distribution under very general conditions—can be regarded as an analogue of the well-known central limit theo-

rem. The central limit theorem states that under very general conditions the distribution of the sample mean converges to the normal distribution as the sample becomes large; the limit represented by Eq. (2) holds for large samples of extremes.

To determine the distribution of the extremes, usually the annual maxima are taken. However, this is only a good choice if the number of realizations within the sampling period (one year) can be considered as asymptotically large, the extremes are independent and identically distributed. As COOK (1982) shows, one may expect that the squared wind speed converges faster than the wind speed itself to the GEV distribution. This assumes a fast convergence for the surge (as it is proportional to u^2).

For estimating the three parameters, the method of Probability Weighted Moments (PWM) was used. The covariance matrix is given by HOSKING *et al.* (1985), from which the uncertainty was estimated by use of the following estimator:

$$\sigma(y, y) \approx \sum_{i=\mu, \alpha, \theta} \sum_{j=\mu, \alpha, \theta} \frac{\partial y}{\partial i} \frac{\partial y}{\partial j} \sigma(i, j) \quad (6)$$

with $\sigma(i, j)$ the covariance of i and j , and $\sigma(i, i)$ the variance. The derivatives of y follow from the inverse of Eq. 3:

$$y = \mu + \frac{\alpha}{\theta} (1 - e^{-\theta x}) \quad (7)$$

Set-Up of the Numerical Experiment

184 runs of 30 years each were generated, with a CO_2 concentration according to the period 1960–1989. This is called the ‘control run’. For each of these ensemble runs, the same initial condition is used for the ocean and the atmosphere except for a random perturbation in the initial potential vorticity field of the atmosphere. This leads to different realizations after several days and hence to other 30-year series representative for the 1960–1989 period (see Figure 4). With the control

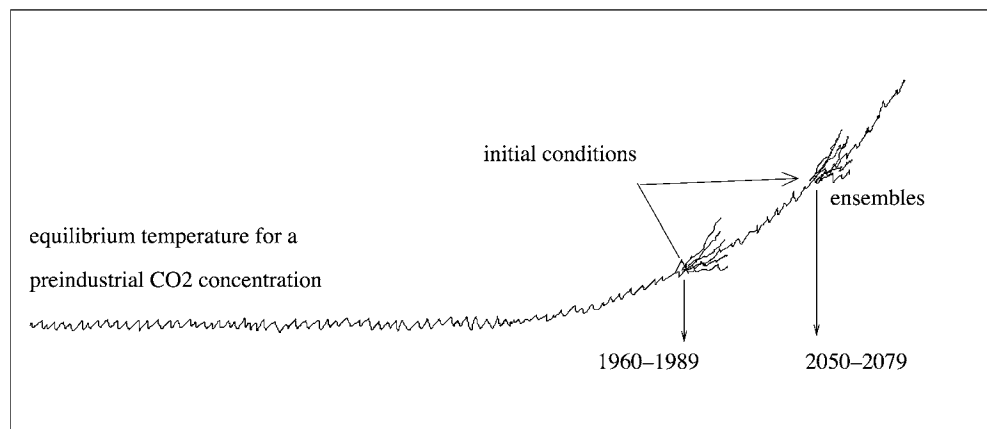


Figure 4. Generating 30-year ensemble runs for two initial conditions. To create the ensembles, small perturbations were adjusted to the initial conditions. The one set corresponds to observed CO_2 concentrations during 1960–1989 and makes the control run, and the other to projected values for 2050–2079, making the greenhouse run.

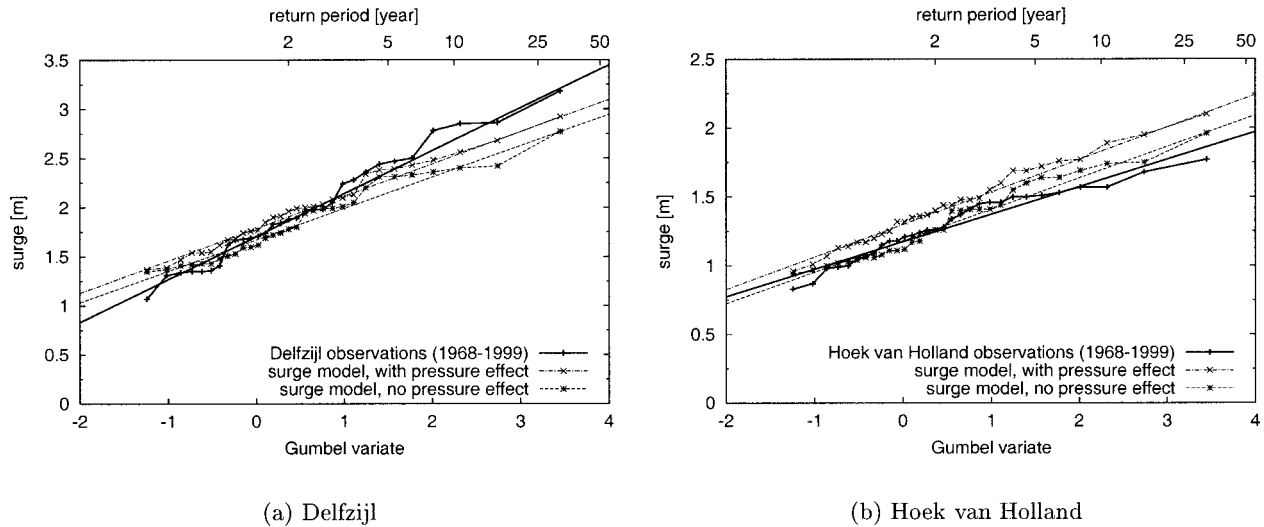


Figure 5. Gumbel plots for the surge in Delfzijl (a) and Hoek van Holland (b), calculated with the surge model (Eq. 1) from the average wind in the North Sea representing NCEP grid points, with and without the local pressure effect. Used is the period 1968–1999. The thick lines represent the fit to the observations.

run, we tested the uncertainty in the extrapolation of the extreme surges for Delfzijl. This was done by deriving the annual extremes from each year, hence one event per year. To ensure independence of the extreme events in two consecutive years, the annual periods run from 1 July to 30 June, giving 29 extremes per ensemble member, and 5336 extremes for the control run. The statistical analysis was performed in three steps: First, the GEV distribution was applied to the total set of 5336 years. From this it was determined whether the full set of the annual surge extremes could be described by a Gumbel distribution ($\theta = 0$) or a GEV distribution with $\theta \neq 0$. Second, the GEV distribution was fitted to the 46 subsets of 116 years each, as the same was done with the observational (118 year) Delfzijl surge record. Third, all 46 estimated 10^4 -year surge levels, and the estimate of the observations, are compared with the estimate of the total set.

Besides the control run, we also generated ensemble runs of 30 year with estimated CO_2 concentrations according to the period 2050–2079 (following the SRES A1 CO_2 emission scenario (HOUGHTON *et al.*, 2001)). This emission scenario results in approximately doubled CO_2 concentration in 2050–2079 (620 ppm on average) with respect to the control run (320 ppm). This ensemble is called the ‘greenhouse run’. Like the control run, it has a total length of 5336 years. We compared the full greenhouse run with the full control run to investigate a possible influence of increased greenhouse gas concentrations on the wind climate over the North Sea.

VALIDATION OF SURGE MODEL AND ECBILT

Wind and Surge

For verification of the surge model, we used the reanalysis dataset of the National Center of Environmental Prediction (NCEP), USA (KALNAY *et al.*, 1996). This dataset provides the weather variables on a global $2.5^\circ \times 2.5^\circ$ grid every 6

hours from 1948 up to the present. The NCEP wind at 10 meter is not a directly measured quantity, but derived via a dynamical atmospheric model from the surface pressure and upper layer measurements. The grid point value is representative of the area around the grid point. We verified the statistics of the NCEP wind with the statistics of Dutch coastal stations. It was found that the differences in the distribution of the daily mean wind speed and direction in winter according to the (3.75E, 52.4N) NCEP grid point and the average of two Dutch coastal stations (Hoek van Holland and Vlissingen, both within the area of this NCEP grid point) were not larger than the differences between the stations itself. We conclude that the NCEP wind data is good enough to rely on for this study.

The validity of the surge model is tested for Delfzijl and Hoek van Holland by feeding Eq. 1 with the 12-hourly NCEP wind averaged over 9 grid points over the North Sea (indicated with open circles in Figure 2). These 9 grid points in NCEP cover the same area as a single grid point in ECBilt (bold dots in Figure 2). The Gumbel distribution was applied to the computed annual (July-to-July) surge extremes, and compared with the distribution of the observed extremes. Both records cover the period 1968–1999. Figure 5 shows that, despite all simplifications, the surge model correctly estimates the parameters of the fitted Gumbel distribution. Illustrative is the fact that the model indicates for more than 50% of the years the correct day at which the annual maximum occurred. Figure 5 also shows that the effect of pressure on the extreme surges has indeed a constant value of only 10 cm throughout the entire range of the extremes. This justifies the neglect of the pressure effect in Eq. 1.

ECBilt Winds

The lowest level of the ECBilt output is 800 hPa (corresponding with a mean height of 2 km), whereas the surge

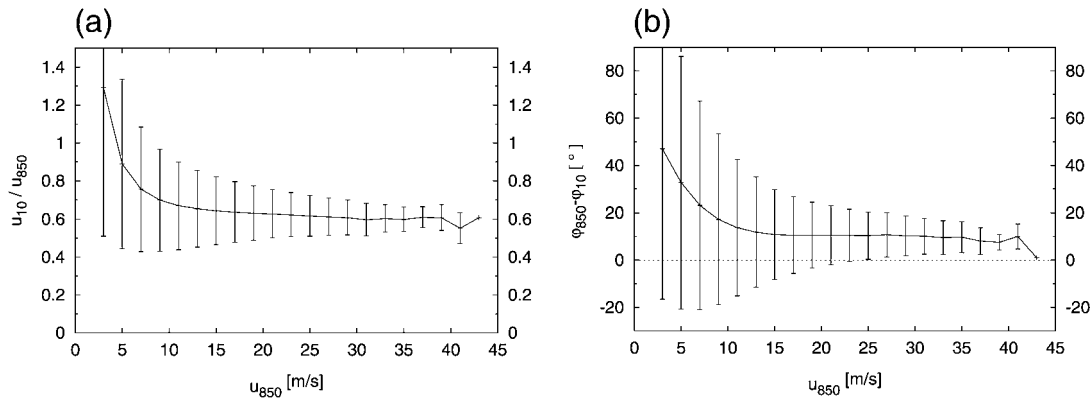


Figure 6. Ratio of the wind speed at 10 m u_{10} to that at 850 hPa level u_{850} (a) and change in wind direction ϕ (b) over sea for the surge-relevant wind directions, for Northern mid-latitudes as derived from NCEP data. The bars indicate the estimated standard deviations.

model assumes 10 meter winds. With the NCEP dataset, we empirically studied the relation between these winds by considering the relation at all NCEP ocean grid points between 40° and 60° North for daily-averaged winds. Figure 6(a) shows the relation between the wind speed at 850 hPa u_{850} and the wind speed ratio u_{10}/u_{850} for the winds between West and North (the relevant directions for positive surges). Figure 6(b) gives the difference in the wind direction between those levels. Both figures indicate a constant value for $u_{850} > 15$ m/s. This constant is 0.6 for the wind speed ratio and 10° for the difference in wind direction, in accordance with GARRATT (1992). From this we conclude that the use of 800 hPa winds instead of 10 meter winds does not influence the shape parameter θ of the GEV distribution, but only the location parameter μ and the scale parameter α .

Figure 7(a) shows the mean geopotential height-field over Europe in winter (Dec–Mar), both for the ECBilt model at 800 hPa and for the NCEP data at 850 hPa and 1000 hPa. There is fair agreement between the ECBilt 850 hPa pattern and the NCEP 1000 hPa pattern, except that the ECBilt pattern is shifted to the south over $5\text{--}10^\circ$. This shift, which is also visible in the standard deviation of the geopotential height (Figure 7(b)), suggests that the wind field over the North Sea is better represented in ECBilt by a somewhat more southerly grid point than by the actual North Sea grid point. Therefore, in our study of surges from the North Sea we considered the grid point (6E, 47°N), indicated in the ECBilt pictures of Figure 7 (see also Figure 2). The fact that this grid point is over land is assumed to be of minor importance, as the ECBilt wind is at 800 hPa, and at that level boundary layer effects can be neglected.

Figure 8(a) compares the distribution of the 800 hPa wind speed and direction (threshold 10 m/s) for this ECBilt grid point of interest (Figure 7) with the North Sea representing NCEP area at 10 meter (open circles in Figure 2). The distribution of the wind speed is represented as a Weibull plot, which results in a straight line if the distribution is described by the Weibull distribution: $F(u) = 1 - \exp(-u/a)^\beta$. The agreement with the NCEP wind speed is good for the wind up to 10 m/s, but deviates for larger wind speeds. This deviation will

lead to a larger location and scale parameter of the GEV distribution. The agreement in direction distributions is less, although the effect of the discrepancy on the surge in Delfzijl (determined by North Western winds) is small. This discrepancy does not play a role in the investigation of the wind speed.

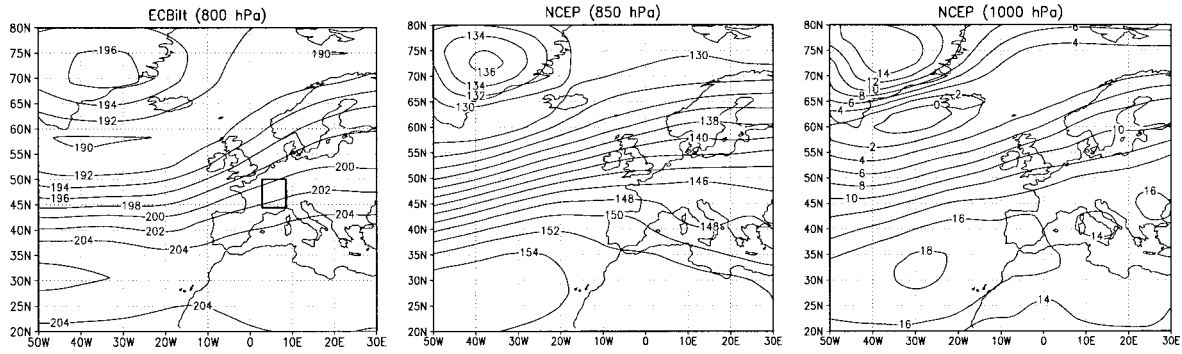
We conclude from this evaluation that the combination ECBilt-surge model seems adequate for the purpose of this study, *i.e.* to explore the uncertainties that are inherent to the determination of 10^4 -year return levels from observational series of 10^2 -year length.

RESULTS

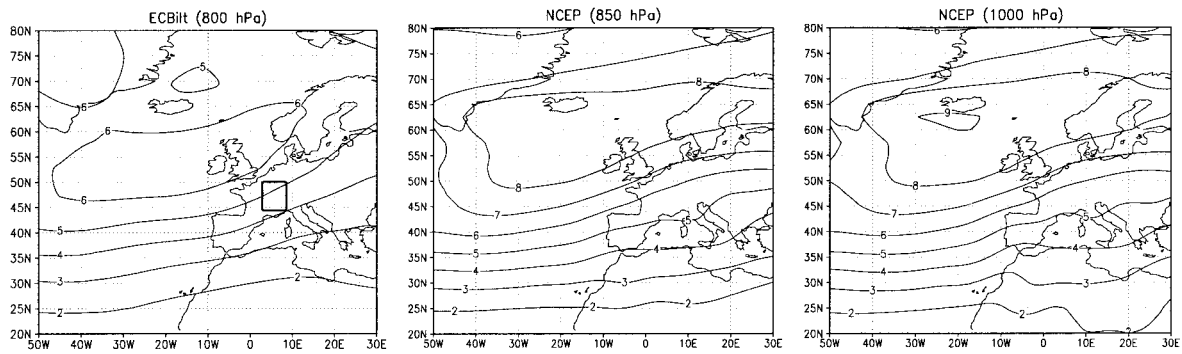
Uncertainty of Estimated Surge Levels

Figure 9 shows the Gumbel plot of the 5336 annual surge extremes of the control run, as calculated from the ECBilt winds by the surge model. The distribution of the annual surge extremes can be described by the Fisher-Tippett II GEV distribution (upward curved, $\theta < 0$), although the largest extremes fluctuate considerably around the fitted line. Up to a return period of 10 years, the extreme surges from ECBilt correspond well with those of the 1881–1999 observational record of Delfzijl. However, the estimated 10^4 -year return level from ECBilt is considerably higher (8.5 m) than from the observational record (5.8 m). This is mainly due to the difference in estimated shape parameters θ (the values are given in Table 1). Figure 9 clearly indicates that a GEV distribution ($\theta \neq 0$) rather than a Gumbel distribution is required to describe accurately the annual surge extremes in ECBilt for the grid point of interest.

Figure 10 shows the histograms of the estimated parameters of the GEV distribution of surges in Delfzijl from all 46 subsets of 116 years of the control run. The mean estimate of the location parameter μ is about 25 cm too low, compared with the observations, which can partly be attributed to the neglect of the pressure effect for the ECBilt extremes. The other parameters to the observational record are in the range of the ECBilt parameters. Noticeable is the wide range in estimated parameters—clearly an effect of sampling. The influence of θ on the estimated 10^4 -year return level is depicted

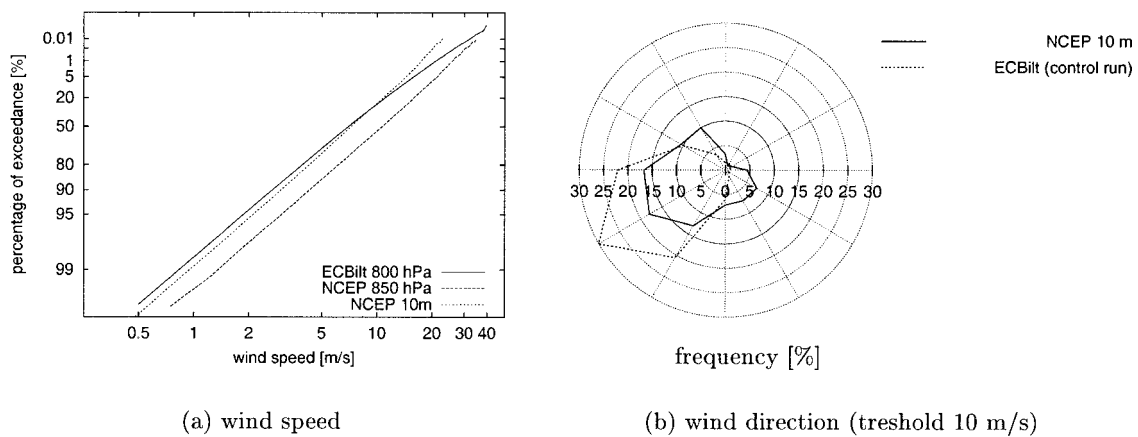


(a) geopotential height (dam) for ECbilt at 800 hPa and NCEP at 850 hPa and 1000 hPa



(b) standard deviation of the geopotential height (dam) for ECbilt at 800 hPa and NCEP at 850 hPa and 1000 hPa

Figure 7. Mean geopotential height over Europe in winter (Oct–Mar) according to a 30-year run of ECbilt at 800 hPa for the control climate, and 30 years of NCEP data at 850 hPa and 1000 hPa (a), with the standard deviation for ECbilt and NCEP (b). The path of the maximum standard deviation is an indicator of the location of the storm track. The grid point in ECbilt, best representing the wind field over the North Sea, is indicated.



(a) wind speed

(b) wind direction (treshold 10 m/s)

Figure 8. Comparison between the considered ECbilt grid point and the North Sea representing NCEP area for the wind speed (a) and the direction (threshold 10 m/s) (b). The wind speed distribution is represented as a Weibull plot. Considered is the winter season (Oct–Mar).

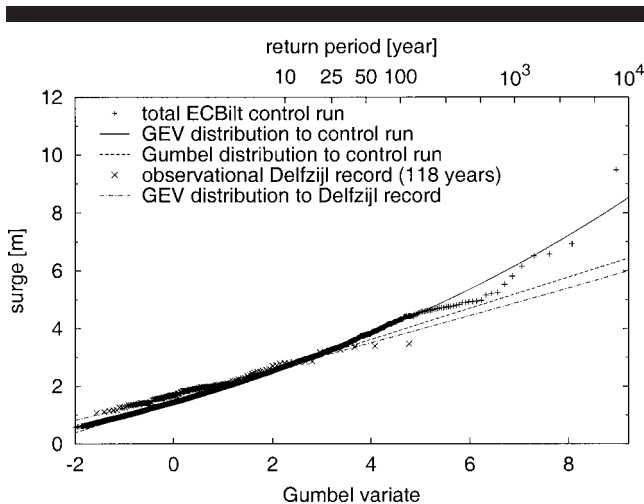


Figure 9. Gumbel plots and fits of the surges for the 5336-year control run in ECBilt for the North Sea representing grid point (6E, 47N) and for the observational record in Delfzijl (118 years). Both the GEV and the Gumbel distribution are fitted to the control run.

in Figure 11, which shows for all 46 subsets the estimated 10^4 -year surge level y_{10^4} as a function of the shape parameter θ . The wide range in θ results in estimated return levels between 4.5 and 17 meters, with an average of 9.2 meter, and a standard deviation of 3.1 meter. These values correspond well with those for the median set ($y_{10^4} = 8.5 \pm 2.7$ m) and the total set ($y_{10^4} = 8.5 \pm 0.4$ m), using Eq. 6 for estimating the standard deviations.

The observational record fits well in the plot, suggesting that this record can be regarded as a realistic subset among all other subsets.

Although Figure 9 indicated that the Gumbel distribution ($\theta = 0$) is not able to describe adequately the annual surge extremes, for 70% of the subsets the hypothesis $H_0: \theta = 0$ is not rejected (at 5% level, according to HOSKING *et al.* (1985)). For most of these situations, the 10^4 -year surge level will be underestimated, giving an average estimate of 8.3 meter instead of 9.2 meter.

In order to find the length of the record required to estimate the 10^4 -year surge level of 8.5 m with an accuracy of 1 meter, we extended two subsets until their estimated 10^4 -year surge levels differed no more than 2 meter. As Figure

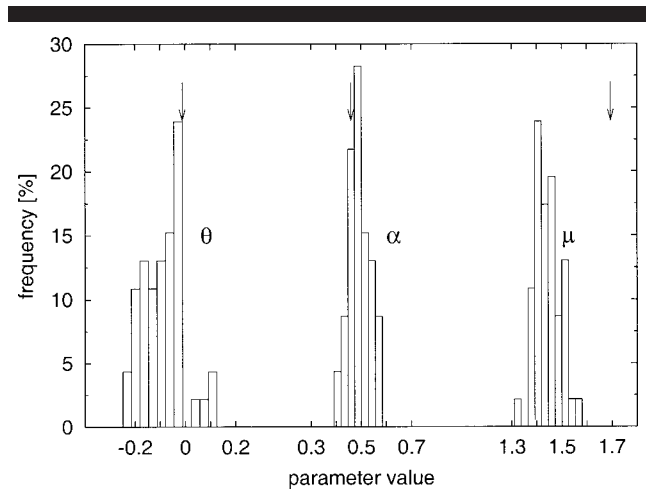


Figure 10. Histograms of the estimated GEV parameters θ , α and μ from the 46 sets of 116 years each from the control run. The arrows indicate the estimates from the 1881–1999 observational set of Delfzijl.

12 shows, in this case the record length should be larger than 10^3 years for an accuracy of 1 meter in the 10^4 -year surge level estimate. Note that also the required record length depends on θ . This dependence is shown in Figure 13 for a relative uncertainty $\sigma(y_{10^4})/(y_{10^4-\mu})$ of 10%. This relative uncertainty is independent of α and μ .

We conclude that the uncertainty in the estimate of the 10^4 -year surge level from a record of 10^2 years is mainly determined by the uncertainty in the shape parameter θ . This uncertainty stems from sampling effects, and leads to an uncertainty of a factor two in the 10^4 -year surge level if determined from the observational record. In practice, a record of order thousand years is required for an uncertainty of 10%.

Greenhouse Effect on Surge and Wind

Figure 14(a) shows a Weibull plot of the distributions of the wind speed for the control run and the greenhouse run for the North Sea representing grid point in ECBilt (6E, 47N). The distributions are virtually identical. The distributions of the wind direction are depicted in Figure 14(b). There is a slight increase in westerly- and a decrease in southerly winds, resulting in increasing frequency of positive surge in Delfzijl.

Table 1 compares the parameters of the GEV distributions

Table 1. GEV-parameters for the fits to the surge (a) and wind speed (b), with the estimated 10^4 -year levels and their uncertainty according to Eq. 6 for the North Sea representing grid point (6E,47N) in ECBilt and for the observational record of Delfzijl. See the Discussion for comments on the uncertainty of the observational record.

	μ	α	θ	10^4 -Year Return Value
(a) surge				
Control run	1.45 ± 0.01	0.49 ± 0.01	-0.091 ± 0.01	8.5 ± 0.4
Greenhouse run	1.57 ± 0.01	0.52 ± 0.01	-0.092 ± 0.01	9.1 ± 0.4
Delfzijl record	1.69 ± 0.05	0.43 ± 0.03	-0.011 ± 0.07	5.8 ± 1.3
(b) wind speed (fitted to u^2)				
Control run	462 ± 2	140 ± 2	-0.069 ± 0.01	47.5 ± 1.0
Greenhouse run	493 ± 2	149 ± 2	-0.053 ± 0.01	47.6 ± 1.0

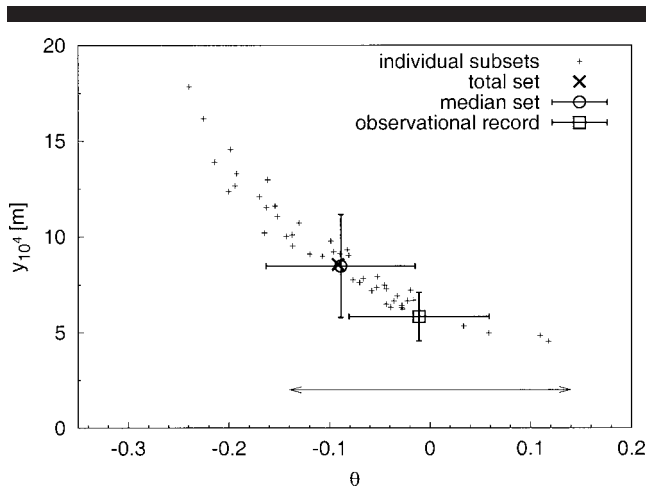


Figure 11. The estimated 10^4 -year return level for the surge as a function of the corresponding θ , together with the estimate from the total control run of 5336 years, and the estimate from the 1881–1991 observational set of Delfzijl, with its standard deviations of θ and the 10^4 -year surge level according to Eq. 6. Also shown is the median set. The arrow indicates the range for which the hypothesis $H_0: \theta = 0$ is not rejected for the subsets (5% level).

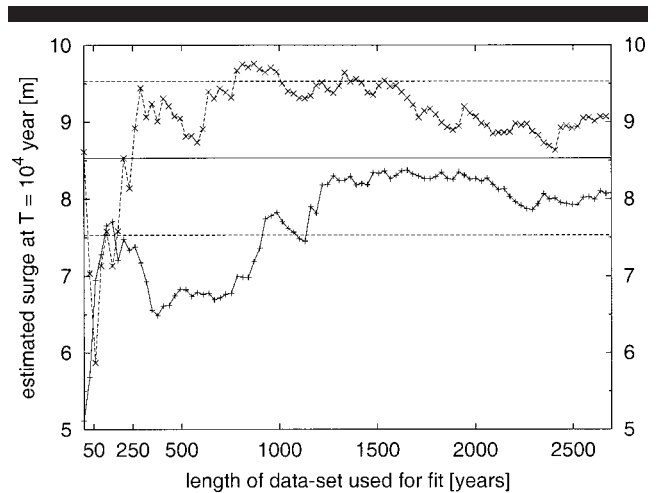


Figure 12. Estimated surge level as a function of the number of years in the data set used for the fit. Shown are two independent realizations from the control run. The estimated value from the total run of 5336 years (8.5 m) is indicated by a solid line. An estimate with an uncertainty of 1 m (dashed lines) requires a record length of order 1000 years.

for the control run and the greenhouse run and the corresponding 10^4 -year surge and wind levels. Figure 15 and Table 1(a) show an increase in the location parameter μ of 8%, and in the scale parameter α of 6% for the surge. The shape parameter θ remains unchanged. This results in an increase of the 10^4 -year surge level of 0.6 meter; this increase is not statistically significant at the 5% level.

The influence of the greenhouse climate on the extreme wind speed is shown in Figure 16 and Table 1(b). Following COOK (1982), the GEV distribution is fitted to u^2 . Like as for the surge, also for the extreme wind speed the location parameter μ and the scale parameter α increase, both with 6%. The (not significant at 5% level) decrease of the shape parameter θ cancels the increase due to μ and α for a return period of 10^4 years.

Figure 16 shows for the greenhouse run a systematic deviation with respect to the fitted distribution for wind speeds with return periods more than 250 years. The kink in the graph, caused by severe events, suggests the existence of a second population in the extreme wind distribution. The fit to the total set is not influenced by these severe events, due to the large number of points before the kink. However, if the sampling period is increased from one year to a century, the parameters of the GEV distribution are predominantly determined by these severe events. Extrapolating from this severe-events-dominated GEV distribution results in a considerably higher 10^4 -year return value for the wind speed than extrapolation of the total set of annual extremes.

DISCUSSION AND CONCLUSIONS

Uncertainty in Extrapolation

The climate model ECBilt indicates that the surge extremes of the control climate can be described with a GEV

distribution up to the return period of interest: 10^4 years. However, the estimates from 46 records of 116 years (like in the observational record) vary between half and twice the median value. This range is also obtained for neighboring grid points, indicating that only a crude estimate can be made with a single record of order hundred years.

For a practical useful uncertainty range of about 10%, one needs 10^3 years of surge extremes. To improve the confidence in the absolute value of the calculated return level, a more complex General Circulation Model has to be used to generate 10^3 years of data for a realistic estimate of 10^4 -year return level of the surge.

Our results suggest that the observational record can be

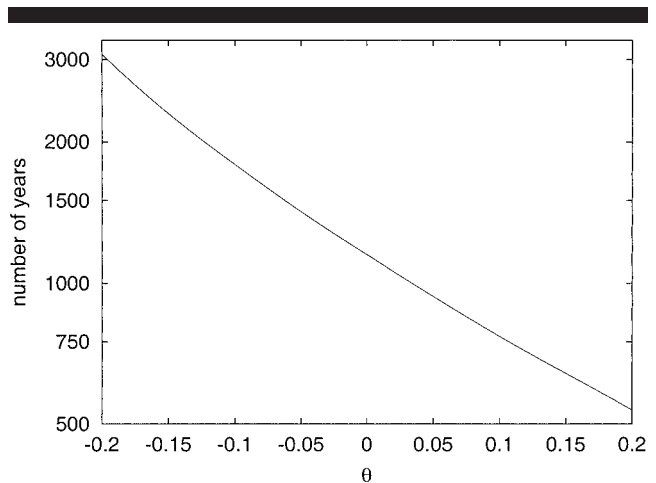


Figure 13. Required record length as a function of the shape parameter θ for a relative uncertainty $\sigma(y_{10^4})/(y_{10^4})$ of 10%, according to Eq. 6. The vertical scale is logarithmic. The required record length decreases quadratically with the relative uncertainty.

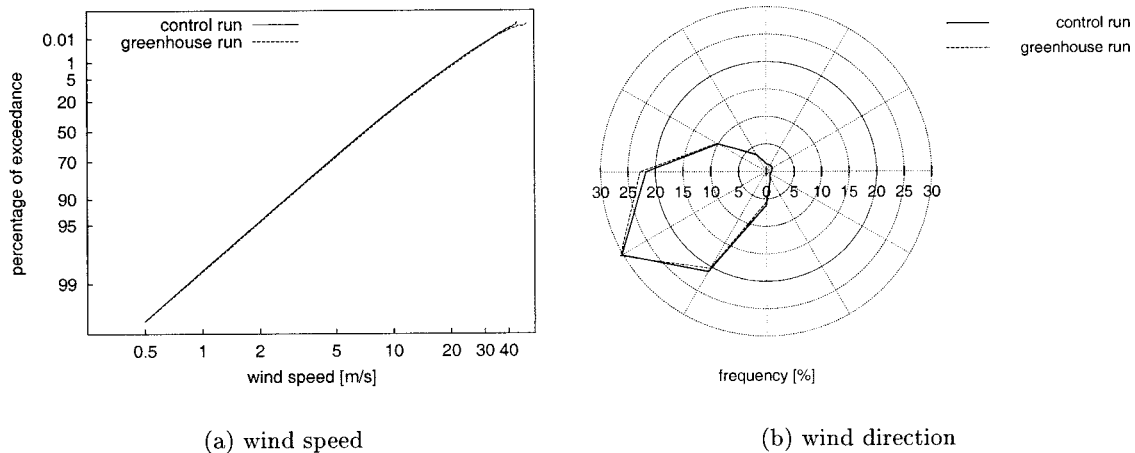


Figure 14. Distributions for the wind speed (a) and the wind direction (b) for the control run and the greenhouse run for the North Sea representing ECBilt grid point (6E, 47N).

regarded as a realistic subset among all other subsets (Figure 10). The considerable lower estimate of the uncertainty range for the observational record ($\sigma(y_{10^4}) = 1.3$ m) than for the ECBilt median set ($\sigma(y_{10^4}) = 2.7$ m) is caused by the non-linearity of y_{10^4} with respect to θ . In the situation of small records (making $\sigma(\theta)$ large) and large return periods (making $(\partial y/\partial \theta)\sigma(\theta)$ dominant over $(\partial y/\partial \mu)\sigma(\mu)$ and $(\partial y/\partial \alpha)\sigma(\alpha)$), a better uncertainty estimate is obtained by determining the upper and lower standard deviations and as $y(\theta - 2\sigma(\theta))$ and $y(\theta + 2\sigma(\theta))$ respectively. Estimating the uncertainty in this way results for the observational record of Delfzijl in an upper bound of 9.2 m, against 8.4 m according to Eq. 6. Monte Carlo simulation gives 9.4 m for the parameters of the observational record. So, Eq. 6 underestimates the upper bound in the situation of short records and large return periods.

The different extrapolation methods, applied to the record

for Delfzijl in DILLINGH *et al.* (1993) show a mutual difference of not more than 10%, whereas the estimates from different records differ up to 200%. This indicates that the method used for extrapolation is of minor importance with respect to accuracy than the representativity of the underlying dataset.

Convergence Rate to GEV Distribution

In this paper we fitted the GEV distribution to the surge and to u^2 . However, it is not known beforehand if these variables are the best choices with respect to their convergence rate to the asymptotic distribution. While theory shows that (for any $k > 0$) the Weibull distribution $F(u) = 1 - \exp(-u^k)$

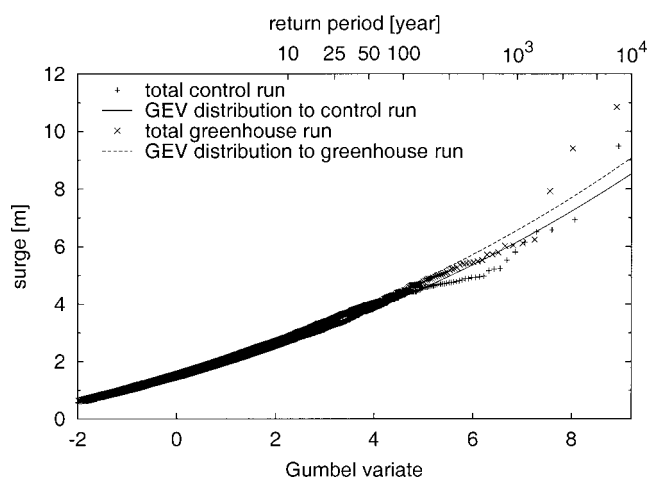


Figure 15. Gumbel plots and fits of the surges for the 5336-year control- and greenhouse runs in ECBilt for the North Sea representing grid point (6E, 47N).

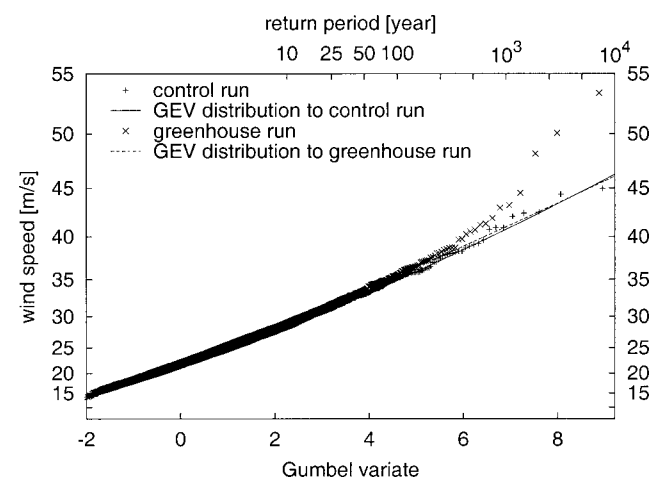


Figure 16. Gumbel plots and fits of the 12-hourly averaged wind speed for the control- and greenhouse runs in ECBilt for the North Sea representing grid point (6E, 47N). The kink at a return period of 250 years in the greenhouse run suggests the presence of a double population in the extreme wind distribution. The vertical scale is quadratic.

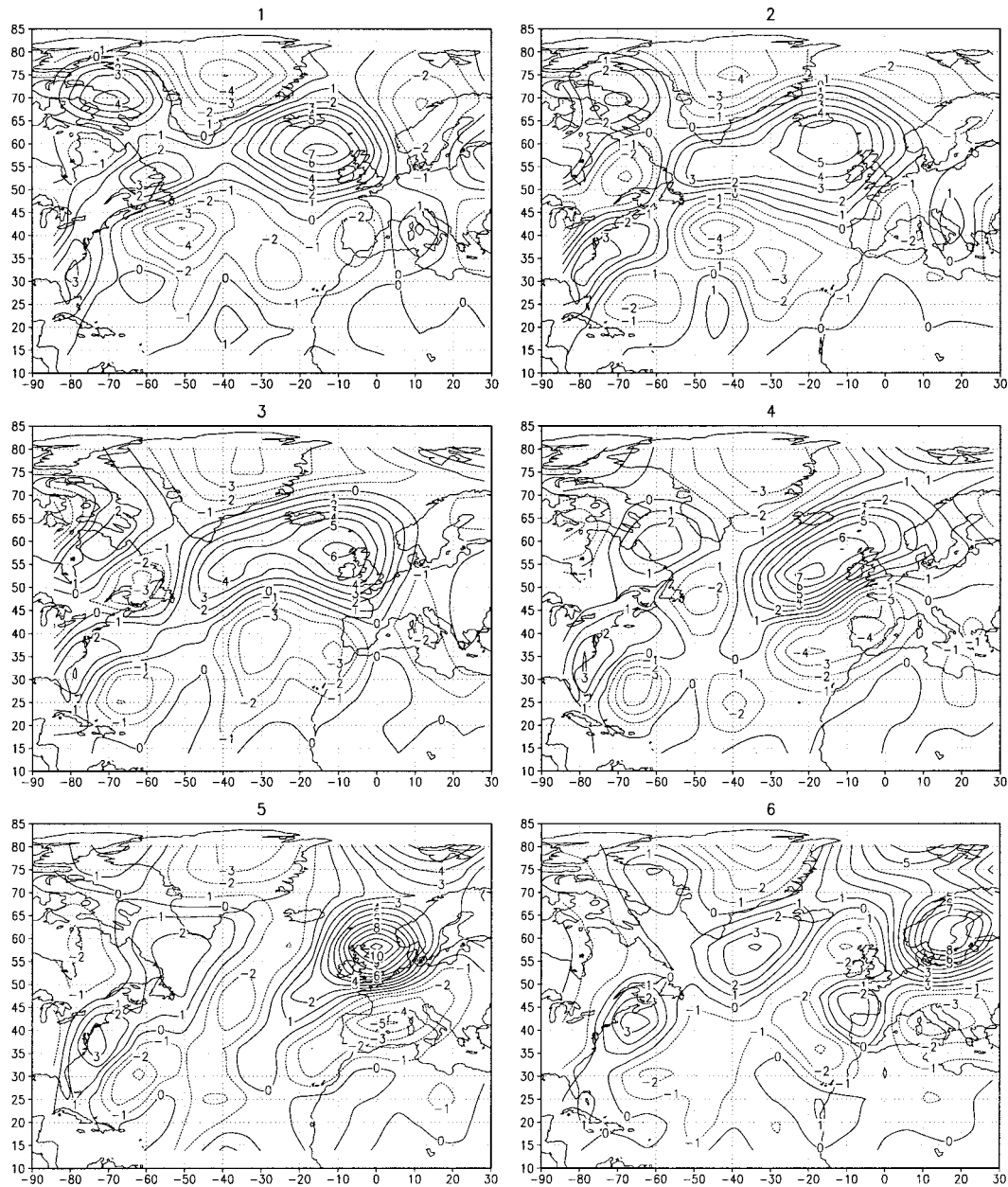


Figure 17. Meteorological situation of a severe ECBilt event. Shown is the daily-averaged vertical component of the relative vorticity (in 10^{-5} m/s^2) at 800 hPa. Panel 5 shows the most extreme situation. The event resulted in a wind speed of 53 m/s, and a surge level in Delfzijl of 7.9 m.

$a)^k$ converges asymptotically to the Gumbel distribution (EMBRECHTS *et al.*, 1997), the convergence rate depends on k . Fast convergence is expected if one fits u^k , with k derived from the tail of wind speed (practically: u larger than Weibull scale parameter a). The reason is that this transforms the Weibull distribution into an exponential distribution, which has a fast convergence to the Gumbel distribution. We therefore recommend to fit u^k , where k can be obtained from Weibull analysis. If a different power n is chosen, then incomplete convergence (due to the finite series length) may result in a over-estimation of θ if $n < k$ and vice versa.

The Weibull distribution of the wind (Figure 14) suggests that in the tail $k \sim 1.5$, which is somewhat smaller than the $k = 2$ -value proposed by COOK (1982). This implies that for wind $u^{1.5}$, or equivalently for surge $y^{0.75}$, has to be extrapolated to get optimal convergence. The incomplete convergence due to the choice u^2 leads to a θ -estimate that is too small. The results on the 10^4 -year level are a 3% smaller wind speed and a 6% smaller surge.

We advice a careful evaluation of the variable to be fitted to obtain fast convergence to the expected extreme value distribution. In any case, one should be careful to interpret $\theta >$

0 as the result of an upper limit, as long as the level of convergence is unclear.

Severe Events

ECBilt hints on the excitation of 'superstorms' in the greenhouse climate, defined as storms with more extreme winds than expected from extrapolation of less extreme events. If these severe events are real, and if they are part of a second population that becomes apparent for high return periods only, than the kink at a return period of ~250 years in the Gumbel plot of Figure 16 means that these 'superstorms' dominate the extreme value statistics at frequencies lower than once in 250 years.

It is tempting to find an interpretation for these superstorms. Preliminary analysis indicates that a part of them may originate from the amalgamation of two precursor cyclones. Cyclogenesis by Wave-Merging is regularly observed above North America (GAZA and BOSART, 1990) but seem rarer above Europe. Merging cyclones are known to result in extreme winds and core pressures (HAKIM *et al.*, 1995a,b).

We speculate at the moment that the changing climate results in a seldom occurrence of these Wave-Mergers over North-western Europe. It may be that this mechanism is also possible in the control climate, but that its rarity is so extreme that it does not show up in the Gumbel plot of order 10^4 year. If this conjecture is true, than the occurrence of superstorms in a greenhouse climate can be regarded to be the result of a increased probability of these events under the changed CO₂ conditions. The time-evolution of the relative vorticity during one of these severe events is shown in Figure 17 (Appendix A). It clearly shows the merging of two cyclones, and the explosive increase in relative vorticity and wind speed.

The reason for this merging, and its relation to the greenhousegas concentration, has to be investigated, as well as the physical reliability of these superstorms. This future research will concentrate on the analysis of the synoptic situations leading to the severe events, and on changes in the spatial distribution of wind extremes due to the greenhouse effect.

APPENDIX A

A Meteorological Situation During a Severe Event

Figure 17 shows the situation from 4 days before till 1 day after the day with the largest wind speed in the ECBilt greenhouse run. The evolution of the daily-averaged vertical component of the relative vorticity at 800 hPa indicates that two storms (with their centers at (55E, 52N) and (15E, 57N) on day 1), interact and merge during day 2 to 5. This results in an explosive increase in relative vorticity and wind speed. The situation in the simulation of Figure 17 resulted in a 12-hourly wind speed over the North Sea of 53 m/s, and a surge level in Delfzijl of 7.9 m.

ACKNOWLEDGEMENTS

We thank T.A. Buishand (KNMI), D. Dillingh (RIKZ), L. de Haan (EUR) and A. Smits (KNMI) for discussions. The

station surge data were kindly provided by J. Doekes (RIKZ). The station wind data were obtained from <http://www.knmi.nl/samenw/hdra/>.

LITERATURE CITED

- BEERSMA, J.J.; RIDER, K.M.; KOMEN, G.J.; KAAS, E.; and KHARIN, V.V., 1997. An analysis of extra-tropical storms in the North Atlantic region as simulated in a control and 2xCO₂ time-slice experiment with a high-resolution atmospheric model. *Tellus*, 49A, 347–361.
- COOK, N.J., 1982. Towards better estimation of extreme winds. *Journal of Wind Engineering and Industrial Aerodynamics*, 9, 295–323.
- DE HAAN, L., 1976. Sample extremes: an elementary introduction. *Statistica Neerlandica*, 30, 161–172.
- DE HAAN, L., 1990. Fighting the arch-enemy with mathematics. *Statistica Neerlandica*, 44, 45–68.
- DELTA COMMISSIE, 1960. *Rapport Deltacommissie*. SDU uitgevers, Den Haag.
- DILLINGH, D.; DE HAAN, L.; HELMERS, R.; KÖNNEN, G.P.; and VAN MALDE, J., 1993. De basispeilen langs de Nederlandse kust; statistisch onderzoek. *Technical Report DGW-93.023*, Ministerie van Verkeer en Waterstaat, Directoraat-Generaal Rijkswaterstaat.
- EMBRECHTS, P.; KLÜPPELBERG, C.; and MIKOSCH, T., 1997. *Modeling External Events*. Berlin: Springer Verlag.
- Galambos, J., 1978. *The Asymptotic Theory of Extreme Order Statistics*. New York: Wiley.
- GARRATT, J. R., 1992. *The Atmospheric Boundary Layer*. Cambridge: Cambridge University Press.
- GAZA, R.S. and BOSART, L.F., 1990. Trough-merger characteristics over North America. *Weather Forecasting*, 5, 314–331.
- HAKIM, G.J.; BOSART, L.F.; and KEYSER, D., 1995a. The Ohio valley wave-merger cyclogenesis event of 25–26 January 1978. part I: Multiscale case study. *Monthly Weather Review*, 123, 2663–2692.
- HAKIM, G.J.; BOSART, L.F.; and KEYSER, D., 1995b. The Ohio valley wave-merger cyclogenesis event of 25–26 January 1978. part II: Diagnosis using quasigeostrophic potential vorticity inversion. *Monthly Weather Review*, 124, 2176–2205.
- HALL, N.M.J.; HOSKINS, B.J.; VALDES, P.J.; and SENIOR, C.A., 1994. Storm tracks in a high-resolution GCM with doubled carbon dioxide. *Quarterly Journal of the Royal Meteorological Society*, 120, 1209–1230.
- HOSKING, J.R.M.; WALLIS, J.R.; and WOOD, E.F., 1985. Estimation of the Generalized Extreme-Value distribution by the method of Probability-Weighted Moments. *Technometrics*, 27, 251–261.
- HOUGHTON, J.T.; DING, Y.; GRIGGS, D.J.; NOGUER, M.; VAN DER LINDEN, P.J.; DAI, X.; MASKELL, K.; and JOHNSON, C.A., 2001. *IPCC Working Group I Third Assessment Report*. Cambridge University Press.
- JENKINSON, A.F., 1955. The frequency distribution of the annual maximum (or minimum) values of meteorological elements. *Quarterly Journal of the Royal Meteorological Society*, 81, 158–171.
- KALNAY, E.; KANAMITSU, M.; KISTLER, R.; COLLINS, W.; DEAVEN, D.; GANDIN, L.; IREDELL, M.; SAHA, S.; WHITE, G.; WOOLLEN, J.; ZHU, Y.; CHELLIAH, M.; EBISUZAKI, W.; HIGGENS, W.; JANOWIAK, J.; MO, K.C.; ROPELIWSKI, C.; WANG, J.; LEETMAA, A.; REYNOLDS, R.; JENNE, R.; and JOSEPH, D., 1996. The NCEP/NCAR 40-year reanalysis project. *Bulletin of the American Meteorological Society*, 77, 437–471.
- KHARIN, V.V. and ZWIERS, F.W., 2000. Changes in the extremes in an ensemble of transient climate simulations with a coupled atmosphere-ocean GCM. *Journal of Climate*, 13, 3760–3788.
- KNIPPERTZ, P.; ULBRICH, U.; and SPETH, P., 2000. Changing cyclones and surface wind speeds over the North Atlantic and Europe in a transient GHG experiment. *Climate Research*, 15, 109–122.
- KOTZ, S. and NADARAJAH, S., 2000. *Extreme Value Distributions: Theory and Applications*. London: Imperial College Press.
- OPSTEEGH, J.D.; HAARSMA, R.J.; and SELTEN, F.M., 1998. ECBilt: A dynamic alternative to mixed boundary conditions in ocean models. *Tellus*, 50A, 348–367.

- OPSTEEGH, J.D.; SELTEN, F.M.; and HAARSMA, R.J., 2001. Climate variability on decadal timescales. *Technical Report 410 200 060*, Dutch National Research Programme on Global Air Pollution and Climate Change.
- SCHUBERT, M.; PERLWITZ, J.; BLENDER, R.; FRAEDRICH, K.; and LUNKEIT, F., 1998. North Atlantic cyclones in CO₂-induced warm climate simulations: frequency, intensity and tracks. *Climate Dynamics*, 14, 827–837.
- TIMMERMAN, H., 1977. *Meteorological Effects on Tidal Heights in the North Sea*. Staats-drukkerij, 's Gravenhage.
- VAN MONTFORT, M.A.J., 1969. Inleiding over de verdeling van extremen. *Statistica Neerlandica*, 23, 97–111.